Exploring the effects of a time- and space-dependent eruption efficiency on planetary evolution in mantle convection code StagYY

Mara Arts

August 19, 2019

Abstract

This project explored the effects of a time- and space-dependent eruption efficiency in planetary convection code StagYY. This has never been considered in a numerical simulation of global mantle convection before. The eruption efficiency gives the ratio of melt that erupts, the rest of the melt intrudes. The eruption efficiency in StagYY has thus far been treated as a constant in time and space. An equation was devised that describes how eruptive a system is, based on the main characteristics of crustal melt transport. These main characteristics are the amount of melt and the local stress state. In this article the effect of this equation is explored with the equation producing results in the background, but still keeping the eruption efficiency that is used constant. This is to find the effects of the equation without it affecting the results of the code. This has shown that the eruptivity of a system is mainly governed by the amount of melt, where the stress has smaller local effects. The eruptivity of a system is mainly governed by the yield stress, eruption efficiency and the viscosity. Parameters that govern the global temperature are less important for the eruptivity. If the eruption efficiency is fully time- and space-dependent the models behave like intrusive systems. The exceptions are resurfacing episodes, these moments are extrusive. Models that show mobile behaviour at almost all times in the planetary evolution will have an almost constant spatially averaged eruption efficiency.

1 Introduction

Magmatism is an important component in the development of planets, since it influences the compositional and thermal evolution (Lourenço et al., 2018; Nakagawa and Tackley, 2012). Two factors are important regarding the composition in the context of melting: the bulk composition and the heat producing elements. Crust is produced from the bulk composition via the separation of minerals during melting. Incompatible minerals enter the melt and leave a depleted mantle behind. Heat producing elements (HPEs) favour the melt, and thus end up predominantly in the crust, this heat released by those HPEs weakens the crust. Especially in young planets the heat production from HPEs is one of the biggest sources of heat (Armann and Tackley, 2012). The influence of melting on the thermal progression comes from the heat necessary to melt the source material. The temperature at the melting location will decrease because of the latent heat necessary to melt the material. The molten material will rise into the crust and will heat the surrounding material. Transport of heat via melt allows for more cooling than heat diffusion alone, resulting in a lower average mantle temperature (Armann and Tackley, 2012) (Lourenço et al., 2018). Melt that is extruded is transported to the surface and cooled quickly to the surface temperature where the heat of melt that is intruded at the base or inside the crust starts heating, and thus weakening, the crust.

The aim of this project is to incorporate a time- and space-dependent magmatism (intrusive or extrusive) in the convection code StagYY and explore the effects of this on planetary evolution. Information about StagYY can be found in section 2.2, Methods. Currently StagYY treats the eruption efficiency, the fraction of melt that erupts, as constant in time and space. It is evident that the eruptivity of a system varies greatly with location; compare volcanic Iceland with northern Japan, where intrusive mafic underplating occurs (Thybo and Artemieva, 2013), and time; in the Archean, Earth was more eruptive than it is today (Mole et al., 2014). It has

been shown that magmatism influences the convection regime (Lourenço et al., 2016), extending the range of yield stresses in which the models show mobile behaviour. An important question of this project is to estimate the importance of density-driven upward melt propagation and the deformation of the crust necessary for the extrusion process to occur. Once a model for the cooling of the propagating melt is formulated, an intrusion/eruption partitioning at each point in the convection domain will be determined. The relative fraction of intrusive and eruptive magmatism therefore will vary laterally, which has never been considered in a numerical simulation of global mantle convection before.

1.1 Lithospheric melt transport

Melt transport in the lithosphere is mainly governed by 3 different processes: porous flow, diapirism and diking. Which of these processes is active mainly depends on the amount of melt and the depth. Porous flow and diapirism are dominant in the deeper parts of the lithosphere where ductile flow is possible, whereas diking is dominant in the shallow lithosphere where there is brittle behaviour (Turcotte, 1987; Petford et al., 2000). Melting and subsequent transport influences the temperature, the composition and the distribution of radiogenic elements in the upper mantle and crust. The main characteristics of diapirism, porous flow and diking are highlighted in the rest of this section.

Diapirism
Diapirism is characterised by hot material that slowly rises through the lithosphere because of a density contrast between the diapir and the host material, causing the buoyant diapir to rise. In diapirs the liquid and the matrix ascend together (Scott and Stevenson, 1986). The heat of the diapir will soften the wall rock, allowing for deformation to make room for the rising diapir. The diapir itself loses a lot of heat in this process, which results in a thermal death for most diapirs in the middle crust (Clemens and Mawer, 1992; Weinberg and Podladchikov, 1994). Diapirism is unlikely to produce extrusive magmatism by itself, but it can transport a large amount of melt into shallower regions of the crust. Diapirs can have ascension rates of up to 100 metres per year (Weinberg and Podladchikov, 1994; Mahon et al., 1988).

Porous flow
Porous flow is the buoyancy driven upward movement to regions with lower pore pressure of melt through pores in the host rock. Porous flow of buoyant liquid through partially molten rock is regarded as the initial transport process leading to melt segregation in the mantle (Scott and Stevenson, 1986). It can occur in regions with lower melt-fractions than those needed for diapirism. The melt loses heat to the host rock while flowing. Porous flow is only feasible in regions with temperatures close to the liquidus. This means that porous flow is mainly important in hot regions in the mantle and lower crust. How far the melt can flow depends on the porosity of the rock and the viscosity of the melt (Turcotte and Ahern, 1978). Porous flow generally has velocities of centimetres per year (Scott and Stevenson, 1986).

Diking
Diking is characterised by narrow near vertical melt filled fractures. These fractures can transport melt through the brittle crust to the surface. These fractures are either opened by the pressure of the melt exceeding the strength of the rock or they follow preexisting faults. The main factors driving the opening of dikes are the melt pressure, the yield stress and the stress state perpendicular to the dike. In the case of vertical diking this would be the horizontal yield stress (Havlin et al., 2013). The pressure at the tip of a dike is the result of the buoyant rise of the melt, minus effects within the dike like viscous resistance. Viscous resistance is affected by the fluid volume, viscosity and dike width. (Havlin et al., 2013). Melt in dikes can rise with velocities of meters per second (McKenzie et al., 1992; Petford et al., 1993).

The common denominator in these three types of lithospheric melt transport is buoyancy. All melt transport is at its core buoyancy driven. So buoyancy should be the main driver when determining how eruptive a system is. The brittle domain in the upper crust is another barrier that the melt needs to overcome before it can erupt at the surface. Since diking is the only important transport mechanism in the upper crust, the driving factor that allows for diking should also be included. This should be a combination of the yield stress and the stress state of the crust, since these govern the strength of the crust that needs to be overcome to initiate diking.

2 Methods

2.1 Rationale

The numerical aim is to find what fraction of the melt will be eruptive at a given location and time in the code StagYY. Since all melt above a certain depth will either extrude or intrude, the intrusive fraction can be found from the extrusive fraction. Melt transport in the ductile regions of the lithosphere is derived from concepts of diapirism and porous flow whereas melt transport in the brittle regions is derived from concepts of diking. The most important concept in all of these regions is buoyancy driven rise. If in the brittle regions the pressure from the melt plus the horizontal yield stress exceeds the local yield stress ($P_m+\sigma_{xx} > \sigma_{ys}$) a dike opens, allowing for continued buoyant rise of the melt through the crust. A very simplified model of melt transport in the crust captures the basic characteristics: the buoyancy driven rise and the the relation between the yield stress and the horizontal stress. To translate these characteristics into a number that represents the fraction of material that will erupt, an equation that uses these characteristics in a balanced way is needed. The output of this equation, to which in the rest of this article will be referred to as eruptivity, is a measure of how eruptive the system is. Melt transport occurs on timescales of months to centuries (Petford et al., 2000), while the shortest timesteps in StagYY represent thousands of years. Since melt transport is instantaneous compared to the timescales used in StagYY, the eruptivity has to be calculated within one time-step.

The range of values of the eruptivity will be explored numerically for various tectonic regimes. Using this range the values of eruptivity in the fully eruptive and fully intrusive scenario are determined. All values in between these extremes will be a linear interpolation between the minimum and maximum value. Additionally applying the eruptivity equation to a known geological system will give another outlook on the fully eruptive values of eruptivity.

2.1.1 Buoyancy

Melt pressure is the result of the pressure of the melt when it rises buoyantly through the lithosphere. The melt pressure at the surface is the combined force of all the melt below that point that could erupt, if a continuous channel is assumed. In the case of StagYY this is all the melt in the lithosphere. For now the rise is simplified to simple buoyant rise based on the density contrast with no regard for porosity, dike width, viscosity of the melt or other complicating factors. Buoyant rise is determined by the density difference between the host rock and the melt. The melt is generally less dense than the surrounding material and will try to rise in the crust. This buoyant rise puts pressure on the rock directly above: the melt pressure. Buoyant rise of the melt is expressed in equation 1.

$$P_{\mathrm{m}} = \int_{z_l}^{0} g f_{\mathrm{m}} (\rho_{\mathrm{s}} - \rho_{\mathrm{m}}) dz \qquad (1)$$

where f_m is the fraction of the rock that has melted at that depth.

The eruptivity should incorporate all the melt that could possibly erupt. For the melt pressure term in describing how eruptive a system is this means that the melt pressure at the surface has to be used. More melt should lead to a more eruptive system since there is more energy available to create the pathway (dikes and diapirs) to transport melt to the surface. Colon (2018) has shown numerically that the eruptive fraction is higher if the eruption rate is higher which in turn is higher if there are higher melting rates. Since the melt pressure is directly linked to the amount of melt this means that a higher melt pressure also should correspond to a more eruptive system. In the cases displayed in this article the melt was always less dense than the host material since it consisted of basaltic melts derived from a harzburgite source material. A basaltic melt is less dense than both basaltic crust or depleted mantle rock in the same pressure temperature conditions. If more complex compositions are used the melt might be less dense than the host-rock in some regions of the crust. If this is only the case in a small portion of the crust some of this melt can still erupt since the pressure from the melt below can push the melt through this region. Equation 1 allows for this behaviour by using a depth dependent density of the host rock. The density of the melt used in the melt pressure equation is the density of the melt at the location where it enters the eruptive/intrusive system. This integral is calculated per vertical column, where it is assumed that there is no horizontal flow of magma between the columns. The melt pressure is the result of all the melt in the column below, which means that uninterrupted flow is assumed. This can only be true if the melt pressure is high enough to initiate diking. This can be simulated by introducing a term that incorporates the local stress state in the brittle domain. This term is explained in the next section.

2.1.2 Local stress state

Next to the buoyancy the local stress state is important for determining whether melt will erupt

or intrude. The local stress state can inhibit diking and prevent the melt from rising through the brittle crust which is necessary for it to be able to erupt at the surface. Diking occurs if the local stress state plus the melt pressure exceed the yield stress. The equation that relates the local stress state to how eruptive a system is should include both the local stress matrix and the yield stress. Not the whole stress matrix is needed however; diking is a mainly vertical feature so it is the maximum compressive horizontal stress that would inhibit diking which is in 2D σ_{xx}.

The yield stress in StagYY is given by two equations: the brittle yield stress (Equation 2) and the ductile yield stress (Equation 3), where $\sigma_{\mathrm{br}}(z_0) = 1e6$, $d\sigma_{\mathrm{br}} = 0.01$ and $\mu = 0.4$.

$$\sigma_{\mathrm{yld}} = \sigma_{\mathrm{br}}(z_0) + P_{\mathrm{dyn}} d\sigma_{\mathrm{br}} \tag{2}$$

$$\sigma_{\mathrm{yld}} = \sigma_{\mathrm{dt}}(z_0) + P_{\mathrm{dyn}} \mu \tag{3}$$

At each point the yield stress with the lowest value will define the local yield stress. This yield stress is almost constant in time and space. The only term that varies is the dynamic pressure P_{dyn}, and its variation is negligible compared to the variation in the stress.

An equation that incorporates both the local horizontal stress and the yield stress would be:

$$\mathrm{stressterm} = \frac{1}{z_c} \int_0^{z_c} \frac{\sigma_{\mathrm{ys}} - \sigma_{\mathrm{xx}}}{\sigma_{\mathrm{ys}}(z_c)} dz \tag{4}$$

This equation will from now on be referred to as stressterm. The stressterm incorporates both terms and ensures that the outcome of the equation is not inherently yield stress dependent. This independence is achieved via dividing by the yield stress at the bottom of the crust. Note that this equation integrates over the thickness of the crust, and not just the brittle domain in which diking occurs. This extended domain is chosen for numerical reasons; the brittle region will in most locations comprise less than one cell. This means that numerical integration is not possible. The stressterm equation still has the numerical problem that the crustal thickness in some regions comprises less than one cell. In these scenarios the system is directly given an eruption efficiency of 1. The eruption efficiency in these places mainly matters for the cooling mechanism that is applied to the melt. In the eruptive scenario the melt is directly cooled to surface temperature, where the melt in the intrusive case is only cooled adiabatically. There should not be a big difference in location between placement at the top or the bottom of the crust since the crust is very thin or non-existent. It is chosen to treat the melt as fully eruptive in these locations as if the crust is very thin the melt can quickly cool to the surface temperature. The adiabatic cooling that corresponds to the intrusive scenario would leave the melt too warm to be representative of these surface or near surface conditions.

f_m	Melt fraction [-]
g	Gravitational acceleration [m/s^2]
P_m	Melt pressure [Pa]
P_0	Reference pressure [Pa]
ρ_m	Density of the melt [kg/m^3]
ρ_s	Density of the solid [kg/m^3]
σ_{xx}	Horizontal stress [Pa]
σ_{ys}	Yield stress [m]
z_0	Surface depth [m]
z_c	Crustal thickness [m]
z_l	Lithospheric thickness [m]

Table 1: Parameters used to calculate the eruptivity

2.1.3 Eruptivity

The final equation that combines both the melt pressure and the stressterm to calculate the eruptivity is the following:

$$\mathrm{eruptivity} = \frac{P_{\mathrm{m}}}{P_0} * \mathrm{stressterm} \tag{5}$$

Or with equations 1 and 4 substituted:

$$\mathrm{eruptivity} = \frac{P_{\mathrm{m}}(z_0)}{P_0 z_c} \int_0^{z_c} \frac{\sigma_{\mathrm{ys}} - \sigma_{\mathrm{xx}}}{\sigma_{\mathrm{ys}}(z_c)} dz \tag{6}$$

The melt pressure is non-dimensionalised using P_0 which will be set to 10MPa for all of the results.

The eruptivity itself does not represent an eruption efficiency. To find the eruption efficiency two extreme values of the eruptivity are chosen; one that corresponds to a fully extrusive scenario ($\mathrm{er}_{\mathrm{erupt}}$) and one that corresponds to a fully intrusive scenario ($\mathrm{er}_{\mathrm{int}}$). All values of the eruptivity are linearly interpolated between this minimum and maximum: $\mathrm{er}_{\mathrm{int}}$ and $\mathrm{er}_{\mathrm{erupt}}$. This gives a number between 0 and 1 that represents the eruption efficiency (ee) of the melt.

$$\begin{aligned} \mathrm{ee} &= \frac{\mathrm{eruptivity}}{\mathrm{er}_{\mathrm{erupt}} - \mathrm{er}_{\mathrm{int}}} - \frac{\mathrm{er}_{\mathrm{int}}}{\mathrm{er}_{\mathrm{erupt}} - \mathrm{er}_{\mathrm{int}}} \\ \mathrm{ee} &= \min(0), \quad \mathrm{ee} = \max(1) \end{aligned} \tag{7}$$

2.2 StagYY

StagYY is a widely used program developed at ETH Zürich used to compute planetary evolution models. StagYY solves the conservation

equations for mass, momentum and energy in Cartesian or spherical coordinates. Melting and crust production is implemented in StagYY. Material in StagYY starts melting if the temperature exceeds the solidus, with the material being fully molten once the temperature reaches the liquidus. The amount of melt is computed at every timestep. The melt that is created is fully basaltic and only the melt above 300km depth is extruded or intruded. A percentage of this melt is extruded while the rest is intruded. Melt is extruded via transporting the melt to the surface and cooling it to the surface temperature. The fraction that intrudes is placed at the bottom of the crust and is only cooled due to adiabatic decompression. Systems that are dominantly intrusive will have a warm lithosphere. For more details on the code StagYY, the reader is referred to (Tackley, 2008), more about melting in StagYY can be found in (Lourenço et al., 2016). All the results were generated on a grid of n_x x n_z = 256 x 64.

3 Results

The testing of the eruptivity equation consisted of two parts. In the first part the behaviour of the eruptivity is examined while the code still has a constant eruption efficiency. In the second part equations 6 and 7 are activated where er_{int} and er_{erupt} are found based on the range of values of the eruptivity in the first part.

All the variables of which the effect on the eruptivity was investigated can be found in Table 2. Not all possible combinations in this table were explored. Instead a few default cases were altered. These default cases are denoted in blue in Table 2. The yield stress, $\sigma_{ys}(z_0)$, has three default cases that roughly correspond to three different tectonic regimes; 10MPa for mobile, 80MPa for episodic and 300MPa for stagnant. A difference in regime is expected to have a big impact on how the eruptivity behaves, so all other combinations of variables should be examined for all of the three regimes. A similar reasoning can be applied to the eruption efficiency (ee). A system that is fully eruptive (ee=1) behaves differently to a mostly intrusive system (ee=0.2) so all parameters should be checked against both an extrusive and an intrusive system. Of all the variables in Table 2 the meaning is explained in the following sections. As well as the effect of that variable on the eruptivity and how this effect is expected to affect the runs where the eruptivity is time- and space-dependent.

Using the er_{int} and er_{erupt} found in the variable testing phase the eruptivity is activated in the second part of the project. This means that

$\sigma_{ys}(z_0)$ [MPa]	10 20 30 50 80 150 300
ee [-]	0.1 0.2 0.3 0.6 1.0
η_0 [Pa s]	1e19 1e20 1e21
T_{CMB} [K]	4500 5000 5500
T_0 [K]	1600 1800 1900 2000
HPE [-]	0.1 0.01 0.001

Table 2: The variables of which the effect on the eruptivity is tested in section 3.1, the blue variables denote the default cases

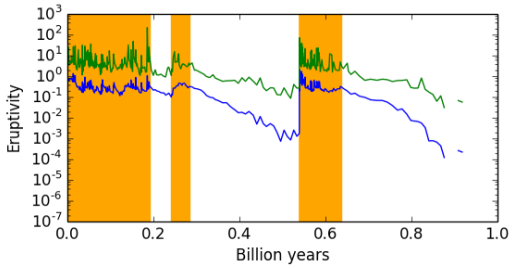

(a) The average eruptivity against time

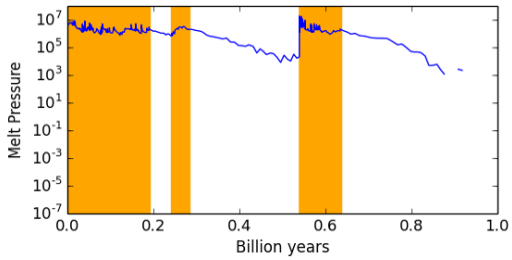

(b) The average melt pressure against time

Figure 1: The melt pressure and eruptivity against time. The yield stress is 80MPa and the eruption efficiency is 0.2. The blue line denotes the spatial average, the green line the maximum found at that time.

the eruption efficiency differs in space and time in the models. A few key models will be rerun to explore the differences that having a variable eruption efficiency makes. Which models will be rerun will depend on the variables that are most strongly affected by having a varying eruption efficiency in the variable testing phase.

3.1 Variable testing

3.1.1 General observations

Before examining the effect of individual parameters, general observations that apply to all of the models will be discussed. A behaviour that is consistent throughout all models is that the mobile moments are more eruptive than the stagnant moments within one model run. Figure 1a shows the eruptivity against time for one of the models. The eruptivity during the mobile pe-

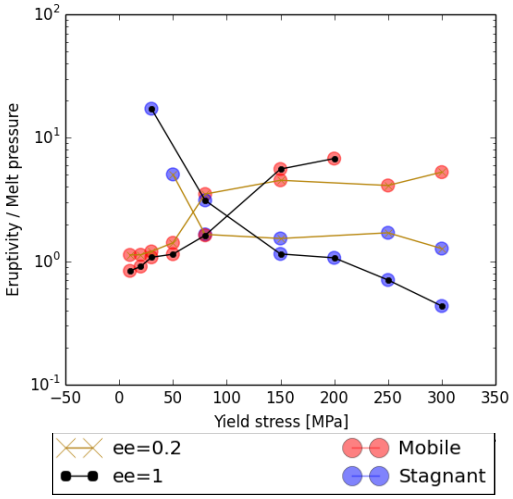

Figure 2: The average eruptivity divided by the average melt pressure in time and space (excluding the first 200 million years) plotted against the yield stress [MPa] for two different eruption efficiencies (ee). Each model run is split in two parts: mobile(red) and stagnant(blue). Mobile represents the average eruptivity of all times where if $V_{rms} >= 1$, stagnant if $V_{rms} < 1$.

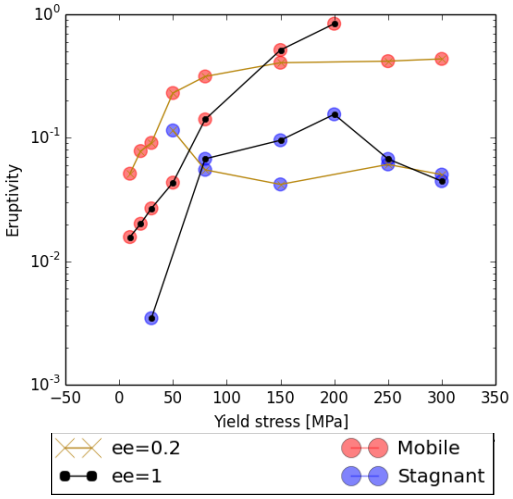

Figure 3: The average eruptivity in time and space (excluding the first 200 million years) plotted against the yield stress [MPa] for two different eruption efficiencies (ee). Each model run is split in two parts: mobile(red) and stagnant(blue). Mobile represents the average eruptivity at all times where $V_{rms} >= 1$, stagnant if $V_{rms} < 1$.

riods, which are denoted with an orange background, is about an order of magnitude higher. This is a direct result of the melt pressure, which also increases during mobile periods; see Figure 1b.

Another observation is that the eruptivity is governed by the melt pressure. Compare the graph that shows melt pressure against time, with the graph that shows the eruptivity against time in Figure 1 and it is unmistakable that both graphs have a very similar shape. Figure 2 was created to find what on average the effect of the stress on the eruptivity for different yield stresses is. It shows the effect of different yield stresses on the average eruptivity divided by the average melt pressure. Each dot represents the average eruptivity in time and space of one model run divided by the average melt pressure. Cells where the crust is thinner than the vertical dimension of the cell are left out of the average. In these cells the effect of the stressterm cannot be calculated. The average eruptivity is split in two parts: mobile and stagnant. The mobile moments represent the times where the surface root mean square velocity is greater than 1 ($V_{rms} >= 1$) for at least 15 million years in a row, the rest of the time is labelled as stagnant. Figure 2 shows that all systems are dominated by the melt pressure, but by how much differs per system. For lower yield stresses especially the stagnant periods get somewhat amplified by the stressterm, where for higher yield stresses not the stagnant but the mobile periods get amplified by the stressterm. Most important is however that the stressterm is on average close to 1. This does not mean that the stressterm can be neglected in the eruptivity equation. Locally the stressterm can amplify the effects of the melt pressure by an order of magnitude.

3.1.2 Yield stress

The surface yield stress referred to in this section is the $\sigma_{dt}(z_0)$ that can be found in Equation 3. Increasing $\sigma_{ys}(z_0)$ increases the overall strength of the lithosphere, making it more resistant to breaking. Models with higher yield stresses will behave stagnant for longer periods because there are higher stresses needed to break the crust. Higher stresses can develop in the lithosphere if it is more resistant to breaking, since for lower yield stress models the lithosphere would have already yielded at these higher stresses.

Figure 3 shows the effect of the yield stress on the average eruptivity. This figure is constructed similarly to Figure 2, except that the average eruptivity is not divided by the average melt pressure. The effect of the yield stress on the eruptivity is different for the mobile and the stagnant times. The spatially averaged eruptivity in the stagnant times does not seem to be affected by the yield stress as can be seen by the limited variation in eruptivity. Especially if the

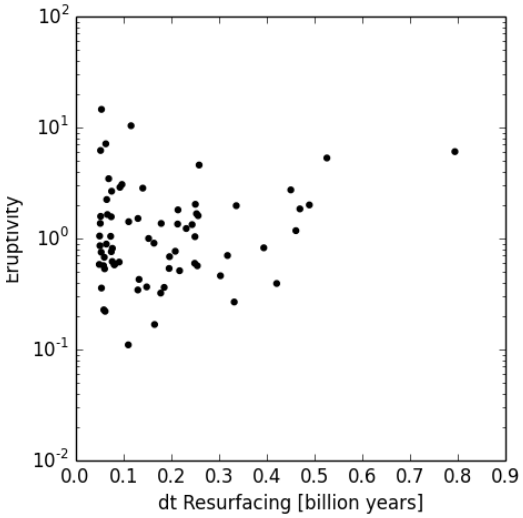

Figure 4: The average eruptivity of a mobile period as a function of the length of the preceding stagnant period. Data from all models is included.

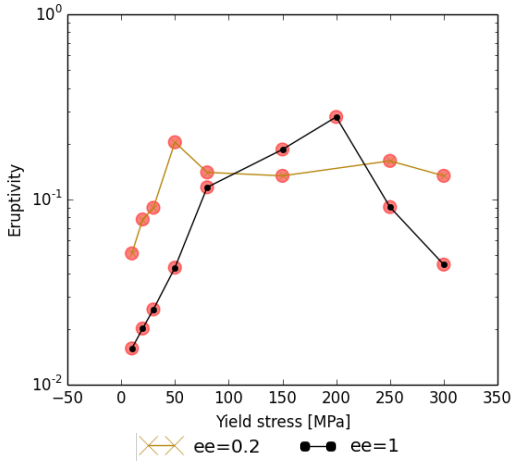

Figure 5: The space- and time-averaged eruptivity plotted against the yield stress.

run with a yield stress of 20MPa and an eruption efficiency is regarded as an outlier, which is not unreasonable since this model was only stagnant for about one percent of the time. Looking at the mobile averages in Figure 3 it is clear that the system becomes more eruptive with increasing yield stress, independent of which eruption efficiency is used. A plausible explanation for this trend could be found in the time between resurfacing events. If the system is stagnant for a longer period more energy remains in the system, which is released during mobile periods. After longer stagnant periods the mobile periods will have more energy, which is translated into more melt. After longer stagnant times the system should be more eruptive. Figure 4 shows the relation between the resurfacing time and the eruptivity. Unfortunately there does not seem to be a correlation between the resurfacing time and the eruptivity. This figure does however include data from runs with a range of different yield stresses and eruption efficiencies. Selecting the data so that it only includes data from the same type of model might show a correlation. This was however not possible with the current dataset, since the amount of resurfacings for runs with similar parameterisations was too limited (only 2 or 3) to be able to observe trends.

Figure 3 does not say anything about how the eruptivity of the total system (i.e. mobile and stagnant periods combined) changes for different yield stresses. Systems with higher yield stresses are stagnant for a larger percentage of run-time. Since these stagnant times are less eruptive the increased eruptivity during the mobile periods is expected to be counteracted by the extended intrusive stagnant periods. If this is the case that would mean that the overall eruptivity of the system is not dependent on the yield stress. Figure 5 shows the relation between the eruptivity and the yield stress for the two different eruption efficiencies. For the fully extrusive scenario there is a large variance in eruptivity for different yield stresses. It is however hard to explain this variance without dividing the model in the mobile and stagnant periods. This is why for the other parameters the effects on the total system will not be discussed.

Systems with a higher yield stress generally develop stagnant systems with a thick crust. Stagnant systems will be mostly intrusive with the eruptivity equation implemented. The heat from the intruded melt will weaken the crust. If the crust is weak enough the convective stresses can be enough to break the crust again, leading to mobile periods. These mobile periods will be more extrusive. This extrusive behaviour leads to a quick accumulation of thick cold crust returning the model to a stagnant period. So for higher yield stresses the eruptivity would favour episodic regimes. The behaviour will not change for low yield stress cases. In these cases the system will always be mobile, this means that the eruptivity will always be the eruptivity that corresponds to the mobile times. This eruptivity does not vary much through time, though there are big spatial differences in the eruption efficiency. These differences are mainly the result of the big local differences in the amount of melt and the stress state. Since the behaviour in scenarios with different constant eruption ef-

ficiencies does not change much, it is not to be expected that there will be big changes with the eruptivity equation implemented.

3.1.3 Eruption efficiency

The eruption efficiency was constant during these model runs. A higher eruption efficiency means that more material erupts. This material is transported to the surface and cooled to surface temperature. The material that is intruded is placed at the bottom of the crust and is only cooled adiabatically. Knowing the effect of a constant eruption efficiency on the eruptivity will tell about how the system will behave when the eruption efficiency is time- and space-dependent.

Figure 6 shows the effect of having different eruption efficiencies on the eruptivity. The variation in eruption efficiency does not have a clear effect on the eruptivity for the stagnant periods. The eruption efficiency does have a strong effect in the mobile periods. What is most striking about the mobile cases is how different the behaviour is for different yield stresses. When considering the 10MPa case, which behaves always mobile independent of the eruption efficiency, it can be seen that the eruptivity decreases with increasing yield stress. If the system becomes more eruptive the eruptivity goes down. If the eruptivity equation was activated in the middle of one of the high eruptivity runs the system would become more intrusive. At this point when the system is more intrusive it would become a bit more extrusive again. This would lead to a balance where the average eruptivity in the end would remain fairly constant through time for the low yield stress scenarios.

The models where the yield stress is 300MPa show the exact opposite trend for the mobile periods. The eruptivity becomes higher with increasing eruption efficiency. This would mean that an eruptive system would stay eruptive or become more eruptive when the eruptivity equation was applied during a model run. Note that these high yield stress scenarios are only mobile for short times during resurfacings. These short times would be very eruptive, and will produce a lot of thick cold crust. This thick cold crust brings the model back to a stagnant behaviour. Implementing the eruptivity equation would thus encourage resurfacing behaviour. The trend that the resurfacings are more eruptive for higher eruption efficiencies could be linked to the length of the preceding stagnant period, since the time between resurfacings becomes longer for systems with higher eruption efficiencies. But as has already been shown in Figure 4 a clear correlation has not yet been found.

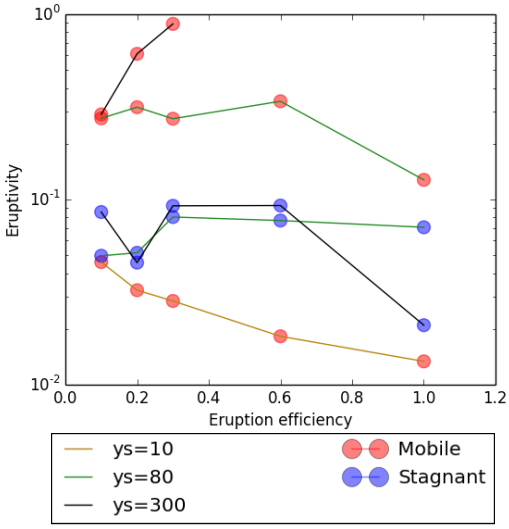

Figure 6: The average eruptivity in time and space (excluding the first 200 million years) plotted against the eruption efficiency for three different yield stresses (ys). Each model run is split in two parts: mobile(red) and stagnant(blue). Mobile represents the average eruptivity at all times where $V_{rms} >= 1$, stagnant where $V_{rms} < 1$.

3.1.4 Viscosity

The viscosity at 1600K and 1Pa (η_0 in Table 2) will change throughout the system based on composition, pressure and temperature. An increase in viscosity will lead to systems that are mobile for a larger percentage of time (Lourenço et al., 2016). Being mobile for a larger percentage of time means for the higher yield stresses that the system will resurface more often. Figure 7 shows the effect of increasing the viscosity on the eruptivity. A higher viscosity will lead to a more eruptive system for the 10MPa and 300MPa cases during both the mobile and the stagnant periods. This could be attributed to the bigger plumes that are being generated when the viscosity is higher (Foulger and Jurdy, 2007). When these plumes reach the surface they generate a lot of melt, which makes the system eruptive. The 80MPa case behaves differently however. The change in eruptivity during the stagnant periods shows a slight upward trend for both eruption efficiencies, but the mobile periods show a slight downward trend. The 80MPa systems do not clearly become more eruptive with increasing viscosity. This could be the result of transitioning from a regime that resurfaces to a fully mobile regime. Regimes that are always mobile generally have a lower eruptivity than

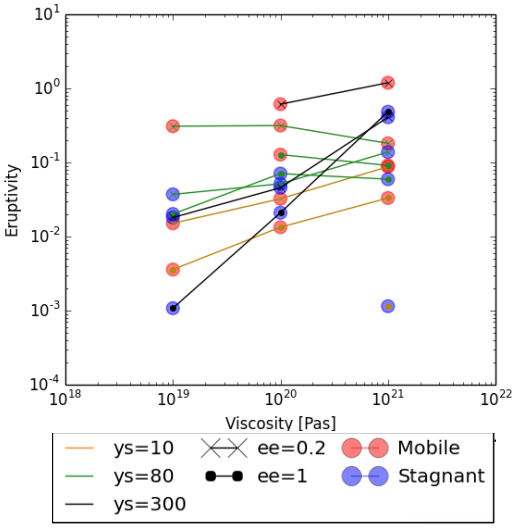

Figure 7: The average eruptivity in time and space (excluding the first 200 million years) plotted against the viscosity [Pa s] for 3 different yield stresses (ys) and two different eruption efficiencies (ee). Each model run is split in 2 parts: mobile(red) and stagnant(blue). Mobile represents the average eruptivity at all times where $V_{rms} >= 1$, stagnant where $V_{rms} < 1$.

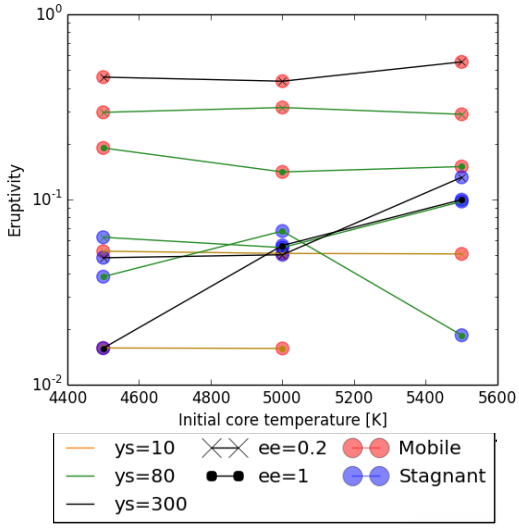

Figure 8: The average eruptivity in time and space plotted against the initial core temperature [K] for 3 different yield stresses (ys) and 2 different eruption efficiencies (ee). Each model run is split in 2 parts: mobile(red) and stagnant(blue). Mobile represents the average eruptivity at all times where $V_{rms} >= 1$, stagnant where $V_{rms} < 1$.

models that show resurfacing behaviour. For the 80MPa case with an eruption efficiency of 0.2 resurfacing occurs for the two lower viscosities, while the highest viscosity is fully mobile. If the eruption efficiency is 1 only a viscosity of 10^{19} is resurfacing and the other two visocisties lead to a mobile system. The effect of a change in tectonic behaviour is thus bigger than the effect of the variation within one type of behaviour.

3.1.5 Core temperature

T_{cmb} is the initial temperature of the core. Since core cooling is activated this temperature goes down during the whole time the model runs. After one billion years the core will have cooled to around 4200K independently of the initial core temperature. The models with higher initial temperature cool more quickly during the first 200 million years. The difference in core temperature after this time is less than 200K. In Figures 2,3,6,7,9 and 10 the first 200 million years are excluded from the averages. For Figure 8 this time is included since most of the effects of varying core-temperatures are included in those first 200 million years.

Figure 8 shows that the initial core temperature does not change the eruptivity of the system during the mobile periods. The stagnant periods do become more eruptive if the initial core temperature is increased. A higher temperature at the core mantle boundary (CMB) will lead to an overall warmer system. This means that during stagnant periods there is more melt, making these periods more eruptive. If core cooling would not be active these effects would most likely have been more pronounced since the temperature difference would have been maintained during the evolution of the model.

3.1.6 Interior potential temperature

The interior potential temperature is more commonly known as the mantle temperature. A higher potential temperature leads to a system with more convective vigour, which leads to systems that show mobile behaviour for longer periods of time.

Figure 9 shows the effect of a higher mantle temperature on the eruptivity of the system. A difference in behaviour can be observed between the 80MPa and 300MPa systems and the 10MPa system. The higher yield stress systems become more eruptive with increasing mantle temperature, where the low yield stress systems seem unaffected by the mantle temperature. The main difference between these cases is that the low yield stress models are mobile throughout the 1 billion year model runs, where the higher yield stress cases resurface. In the mobile cases the planet cools down more quickly than in the stagnant cases, in which the average mantle temper-

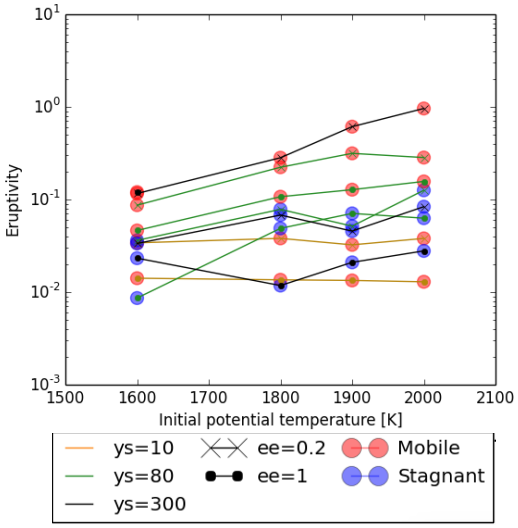

Figure 9: The average eruptivity in time and space (excluding the first 200 million years) plotted against the interior potential temperature [K] for three different yield stresses (ys) and two different eruption efficiencies (ee). Each model run is split in 2 parts: mobile(red) and stagnant(blue). Mobile represents the average eruptivity at all times where $V_{rms} >= 1$, stagnant where $V_{rms} < 1$.

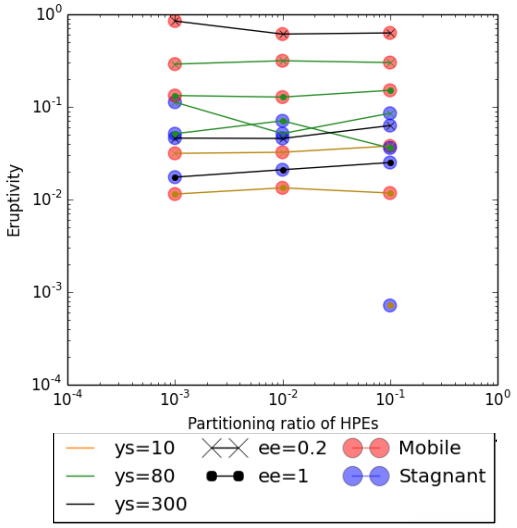

Figure 10: The average eruptivity in time and space (excluding the first 200 million years) plotted against the partitioning ratio of heat producing elements for three different yield stresses (ys) and two different eruption efficiencies (ee). Each model run is split in two parts: mobile(red) and stagnant(blue). Mobile represents the average eruptivity at all times where $V_{rms} >= 1$, stagnant where $V_{rms} < 1$.

ature can even increase over the course of the stagnant periods. A higher temperature results in more melt, which can be seen in a higher eruptivity.

The effect of varying the mantle temperature is less than that of the yield stress, eruption efficiency and viscosity. This is surprising, since in systems that are driven by the melt pressure the temperature is expected to have a large influence because it directly influences the amount of melt. So either a higher mantle temperature only produces so little additional melt that it has no effect on the eruptivity or there are other processes related to the temperature that cancel the effect that larger amounts of melt would have on the eruptivity.

3.1.7 Heat Producing elements

Heat producing elements (HPEs) are elements that produce heat via radioactive decay. Most HPEs are incompatible, which means that they favour going into the melt over staying in the solid when a rock is melting. Since the melt will end up either at the top or the bottom of the crust the HPEs will also be predominately in the crust. This results in a crust that is enriched in radiogenic elements compared to the mantle. The heat from the HPEs will start weakening the crust, making it more vulnerable to breaking. This can be seen in the time that models are mobile, models where a larger percentage of the elements go into the melt show mobile behaviour for a larger percentage of the time. The partitioning coefficient shows the ratio of how likely an element is to go into the melt over staying in the solid. A lower partitioning coefficient means that the element is more likely to go into the melt.

Taking a look at Figure 10 where the eruptivity is plotted against the partitioning coefficient shows that partitioning of HPEs has no effect on the eruptivity. The effect of the heat producing elements might have been overshadowed by the hot setup of the models. The temperature added was irrelevant compared to the initial core/mantle temperature (1900K). Looking at the effects of HPEs with a lower initial temperature might show different results. Unfortunately, such cases are not part of the currently accessible pool of results.

3.2 Mid-ocean ridge

A mid-ocean ridge is a well studied region that can be regarded as fully eruptive. Applying the eruptivity equation to this region will give insights to which value of the eruptivity corresponds to a fully eruptive system.

Since the crustal thickness is around zero at

the centre of a mid-ocean ridge the stressterm will be neglected. This should not cause a big deviation since it has already been shown that the stressterm is of secondary importance to the eruptivity.

Based on a simple corner flow model where both the adiabat and the solidus are linear the melt-fraction will decrease linearly with depth (Langmuir et al., 1992). This yields the following equation for the melt pressure:

$$P_m = g(\rho_s - \rho_m) \int_{z_s}^{0} (1 - \frac{z}{z_s}) dz \qquad (8)$$

Where f_m is substituted with $1 - \frac{z}{z_s}$. It is assumed that the densities of both the solid and the melt are constant and that the rock is fully molten at the surface and fully solid at depth z_s. Inserting densities of $\rho_s = 3000kg/m^3$ and $\rho_m = 2800kg/m^3$ and a z_s of 50km will lead to a melt pressure of around 50MPa. The melt pressure in these models has been normalised using $P_0 = 10MPa$. The eruptivity corresponding to a fully extrusive scenario would hence be 5. This "back of the envelope" calculation only gives the order of magnitude that would be suitable for a fully extrusive scenario. When looking at the plots that show the average eruptivity as a function of the variables this average eruptivity is always in the range of 0 to 1. An er_{erupt} of 1 would make the average never fully extrusive or intrusive. An er_{erupt} of 0 would be suitable since this would correspond to the no-melt scenario. The runs with the eruptivity equation fully active will hence be carried out with $er_{erupt} = 1$ and $er_{intrude} = 0$.

3.3 Time- and space-dependent eruption efficiency

The next section will display the results when the eruptivity equation is active in the code. Figure 11a shows the spatially averaged eruption efficiency as a function of time. This figure shows that the system is more eruptive during mobile moments, as had already been observed during the variable testing phase. After a peak in eruption efficiency during a mobile moment the model slowly returns to be mostly intrusive during the stagnant times.

Figure 11a shows the spatial average of the eruption efficiency as a function of time when the eruption efficiency is time- and space-dependent for different scenarios. For both the fully extrusive as well as the mostly intrusive case the graph shows the eruption efficiencies the system would have had if from that time onward the eruption efficiency would be time- and space-dependent. Comparing Figure 11a with the mostly intrusive (Figure 11b) and fully extrusive (Figure 11c) scenarios, it becomes clear that the time- and space-dependent scenario has a closer resemblance with the intrusive scenarios. The fully extrusive case is characterised by a stagnant behaviour. The mostly intrusive scenario is stagnant for long times and resurfaces sometimes. The time- and space-dependent eruption efficiency (Figure 11a) shows behaviour that is similar to the mostly intrusive case, but it shows a few quick transitions from stagnant to mobile in the first 200 million years. A difference between the intrusive and the time- and space-dependent case would be the difference in amplitude during eruptive moments. The eruptive moments in the time- and space-dependent case are more eruptive and the intrusive moments are more intrusive. After a mobile period the time- and space-dependent case returns more quickly to the lower eruption efficiencies than the intrusive scenario. This is the result of the enhanced crust production in the time- and space-dependent scenario. The extra crust produced during mobile periods forces the system to become stagnant more rapidly. The mobile periods are also shorter for the time- and space-dependent case than for the intrusive one.

The effect of a time- and space-dependent eruption efficiency on the crustal thickness can be seen in Figure 12. What happens in the intrusive case (ee=0.2) is that during the mobile periods crust gets recycled, so the average crustal thickness becomes a lot thinner. With the time- and space-dependent eruption efficiency the crust also gets recycled, but the increased eruption efficiency causes a lot of melt to erupt, which quickly produces a thick cold crust again. This thicker colder crust brings the system back to stagnant. This does not mean however that having an time- and space-dependent eruption efficiency forces the system to be stagnant at all times. The intrusive behaviour during stagnant time heats the crust. This heated crust can be more easily broken, which starts a mobile period.

Figure 13 shows the percentage of time that a model behaves mobile, excluding the first 200million years. Trends that have been observed before, like systems becoming more stagnant with increasing yield stress and decreasing viscosity, are displayed in these plots. These diagrams generalise what was already shown for one example in Figure 11; the system behaves more like the intrusive scenario. What these diagrams show is if the models are stagnant or mobile. The lighter the colour the more stagnant that model run was. Except for the completely white blocks, these represents the points where

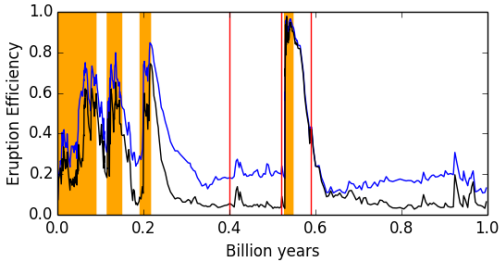

(a) time- and space-dependent, the red lines are the times displayed in Figure 13.

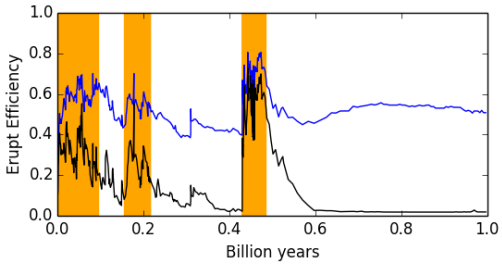

(b) eruption efficiency = 0.2

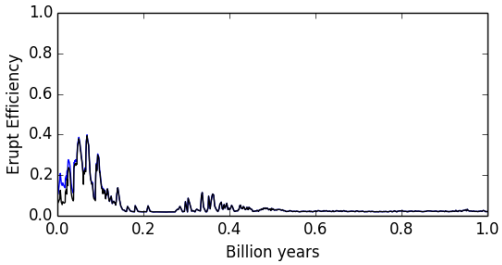

(c) eruption efficiency = 1.0

Figure 11: The spatial average eruption efficiency as a function of time. Orange regions show where V_{rms} at the surface is > 1. The blue line is the total average. The black line is the average of the regions where the crust is thick enough to apply Equation 4. The yield stress used is 300MPa.

there is no data. The time- and space-dependent case is nowhere fully stagnant, the scenario with the highest yield stress and the lowest viscosity still has one resurfacing.

Figure 14 highlights three different times of the model run shown in Figure 11. The outer circle of each plot shows the eruption efficiency at each location, the inner circle the temperature. Figure 14a shows the system while it is stagnant. During stagnant periods the whole system is mostly intrusive, except for a few places where the crust is too thin to apply Equation 4 which are fully extrusive. Figure 14b shows the system just after a big plume arrived at the surface. This plume has produced large amounts of melt, making the system in these places fully eruptive. The rest of the system is, at this point

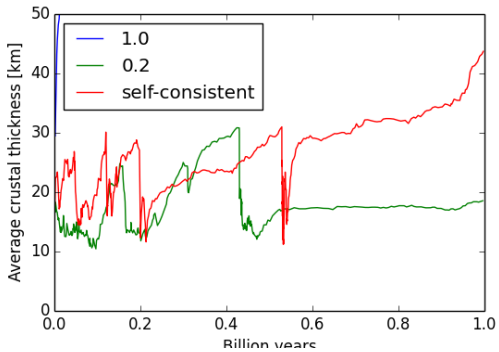

Figure 12: The crustal thickness as a function of time. For the eruption efficiency is 1.0 case (blue line) the crustal thickness exceeds 50km within the first 50 million years.

in time, not affected by the plume and is still mostly intrusive. This plume initiates a mobile period. The last image, Figure 14c, shows the system just after the mobile period, that was initiated by the plume, ended. The mobile moment itself was not shown, during these times there are almost no locations where Equation 4 can be applied. The system is still very extrusive since there is a lot of melt present. How extrusive each location is differs per location. Regions above warmer patches in the mantle can be seen to be more eruptive, where regions that overly a cold lithosphere are mostly intrusive. An interesting local effect has to do with the crustal thickness around regions where a plume arrives. When the plume arrives in these regions the system becomes very eruptive because of the large amounts of melt that a plume generates. This high eruptivity translates into a thick cold crust right above the plume. This thick cold crust does not leave room for melt, forcing the melt to the sides of this thickened crust. This means that directly above the plume the system is quite intrusive and at the edges of the region affected by the plume the system is more eruptive.

All the results with the time- and space-dependent eruption efficiency that have been shown so far described models that showed resurfacing behaviour. Figure 15 shows the eruption efficiency for a run that was mobile. The blue line denotes the average eruption efficiency and the black line the average eruption efficiency where there is enough crust to apply Equation 4. It is apparent that this mobile run has an almost constant eruption efficiency of 0.7. This does not match the findings in the variable testing phase, where it was stated that systems that show mobile behaviour during the whole run period are relatively intrusive. This higher eruption efficiency is the effect of setting

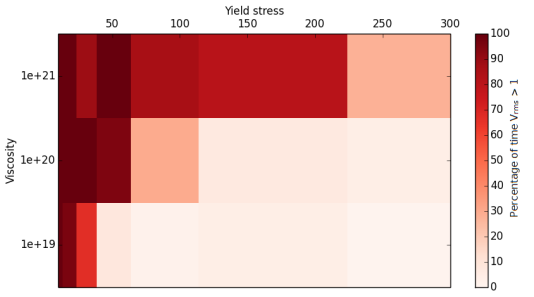

(a) time- and space-dependent

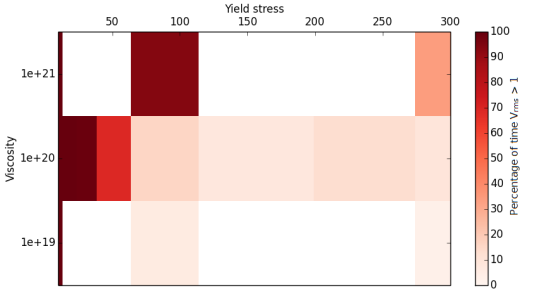

(b) eruption efficiency is 0.2

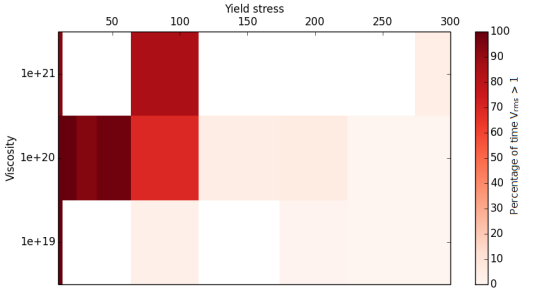

(c) eruption efficiency is 1.0

Figure 13: The percentage of time a model was mobile. The white areas contain no data.

the eruption efficiency to 1 in places where the crust is too thin to apply the stressterm. The black line would be closer to the eruption efficiency that represents the amount of melt in the system.

4 Discussion and conclusion

The goal of this project was to investigate the effects of a time- and space-dependent eruption efficiency in mantle convection code StagYY. This was attempted through the creation of an eruptivity equation, based on the melt pressure and the stressterm. The eruptivity equation (Eq. 6) gives an indication of how eruptive a system is at a given time and place. This equation was created with different transport mechanisms of melt in the lithosphere in mind. This equation correctly predicts that mid-ocean ridges are fully eruptive and that systems with less melt are more intrusive. Based on the eruptivity the extrusion efficiency is determined based upon a linear interpolation (Equation 7).

Melt transport in various systems has been studied extensively. Geochemical and geological (Colon, 2018) global and regional studies, analogue modelling and numerical codes (Havlin et al., 2013; Lourenço et al., 2018). Most of these studies study melt transport in more detail than what has been presented in this article. Though no other study has been able to incorporate a time- and space-dependent eruption efficiency into a global evolution model.

In the eruptivity equation the term that represents the melt pressure is dominant, independent of the behaviour of the model. The stress did however have local influences and hence cannot be neglected. The eruptivity of a system is mainly influenced by the yield stress, the eruption efficiency and the viscosity. Especially the yield stress and the eruption efficiency are closely connected. Increasing the yield stress changes the effect of the eruption efficiency on the eruptivity. It was surprising to see that the effects of the temperature related parameters (the initial core temperature, initial potential temperature and heat producing elements) on the eruptivity are limited. Either an increase in these temperature related parameters does not produce enough additional melt to cause a change in the eruptivity or there are other processes related to the temperature that cancel the effect that larger amounts of melt would have on the eruptivity. If the eruption equation is applied in the models the system will behave like a mostly intrusive system. For models that are continuously mobile the spatially average eruption efficiency is almost constant in time. For the models that were resurfacing the eruption efficiency was low during stagnant periods and high during the mobile periods. This will drive the systems to resurface more often, for shorter amounts of time.

A time- and space-dependent eruption efficiency allows for a more realistic model of planetary evolution. It results in systems that show resurfacing behaviour up to higher yield stresses and these systems resurface more often during shorter periods. A time- and space-dependent eruption efficiency does not have a big impact on models that show mobile behaviour at all times during the planetary evolution. In these models the spatially average eruption efficiency is almost constant. For all models there are differences based on location. Regions above plumes are always more eruptive than regions where there is little melt.

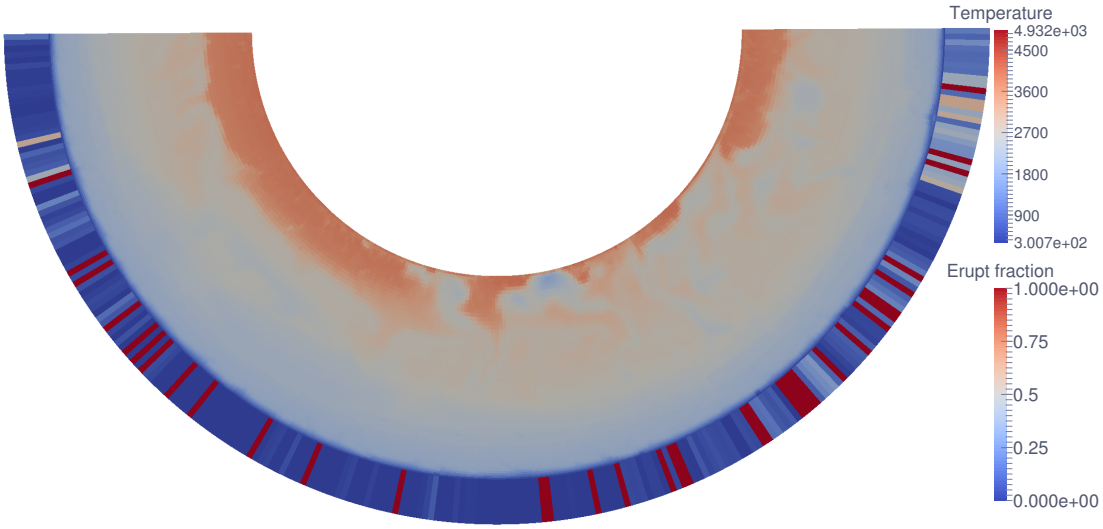

(a) t=0.40 billion years

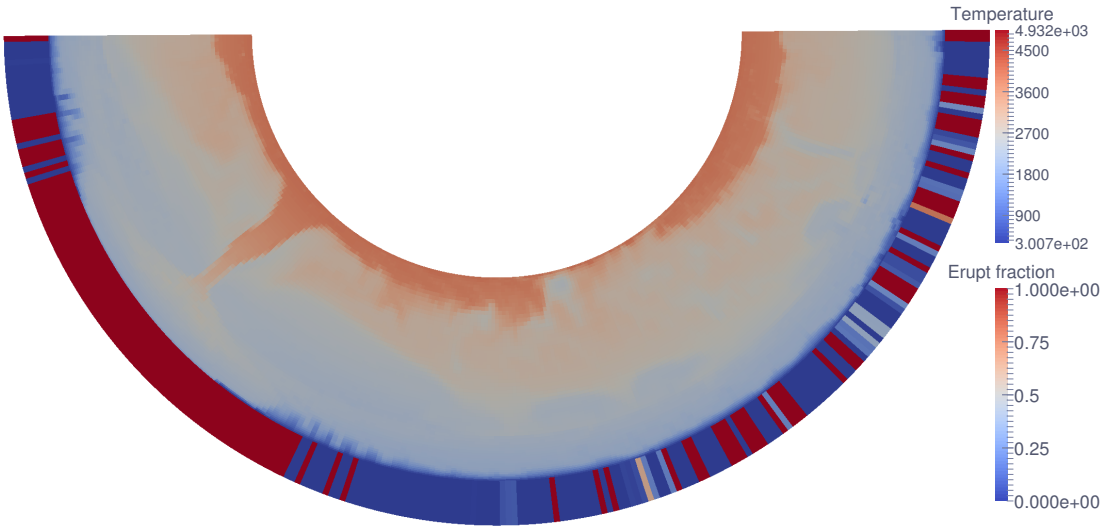

(b) t=0.52 billion years

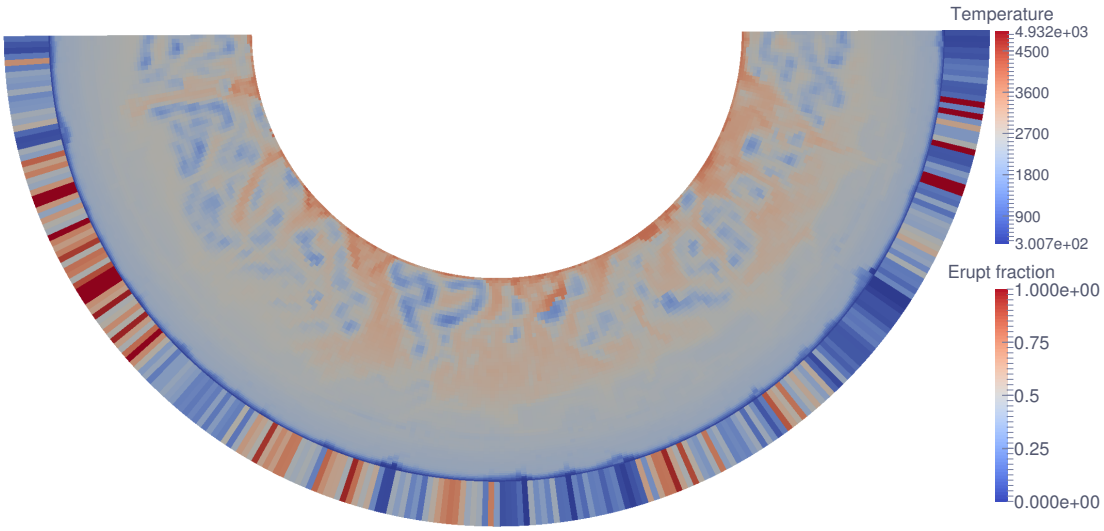

(c) t=0.59 billion years

Figure 14: Three timesnaps from the run highlighted in Figure 11 which has a yield stress of 300MPa.

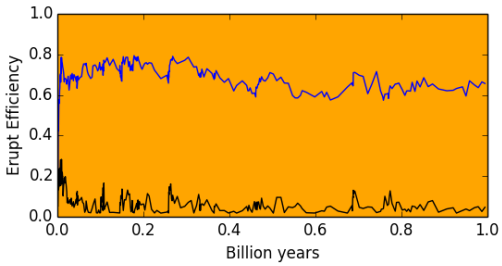

Figure 15: The eruption efficiency of a run with mobile behaviour, the yield stress is 10MPa.

The eruptivity equation takes into account the most important characteristics of melt transport. Some other characteristics that are also important, e.g. the viscosity of the melt, were however left out of this study. A higher viscosity would mean that the pressures necessary to cause yielding should be higher, since flow into the dike is limited if the viscosity is higher (McLeod and Tait, 1999). The viscosity of the melt inherently changes when the melt is cooled during its transport in the crust. Other limitations of the eruptivity equation are numerical in nature. The stressterm should only be applied in regions where there is brittle behaviour in the crust, not the whole crust. Aditionally, if the crustal thickness is less than the thickness of one cell, the eruption efficiency should not be set to 1. This is inherently resolution dependent, which is a characteristic the eruption efficiency should not have. Both of these problems could be solved by changing how the stressterm is handled numerically. The limitation that the crustal thickness should comprise at least one cell comes from the fact that the horizontal stress is only available per cell. This problem could be solved by only applying the melt pressure part of the eruptivity equation in the columns where this poses a problem. Another option is to use the horizontal stress of the whole cell and assume it approaches the horizontal stress in the brittle domain. This assumption is not always valid since the stress changes a lot between different cells, so it is unfair to assume that it would be constant within one cell. However, this approach might still be better than just neglecting the stressterm. The brittle yield stress is the result of Equation 2, so for this equation the pressures should be interpolated to be able to integrate within one cell. Changing this would make the systems less eruptive, since the eruption efficiency will no longer be 1 by default in these problematic regions. If there is no crust at all the eruptivity will remain 1 for the reasons already mentioned in Section 2.1.2.

One question that is left unanswered is why sometimes the stagnant periods are affected, sometimes the mobile periods and sometimes both when varying the parameters in variable testing. This might have a relation to the duration of the stagnant/mobile periods and how the parameters alter the time between resurfacing episodes. This relation is however not clear as shown by Figure 4, maybe filtering the data will show some more trends. This would however need more data with similar settings, since most models now only have one or two resurfacing events and the resurfacing events of models with too different parameterisations cannot be compared. A longer run-time for the models already shown could already prove useful.

It would be interesting to see how the results would change for 3D scenarios. The effect of the melt pressure would probably decrease. In the 2D scenarios each plume effectively acts as a ridge, whereas in 3D they would be a point source. In 3D the stressterm would have to use the minimal horizontal stress. Diking will simply occur along the weakest axes, which is given by the minimal horizontal stress since the yield stress does not change. Additionally it would be interesting to see how a time- and space-dependent eruption efficiency would change models with parameterisations that represent observed planets, like Earth, Venus and Mars.

References

Armann, M. and Tackley, P. J. (2012). Simulating the thermochemical magmatic and tectonic evolution of venus's mantle and lithosphere: Two-dimensional models. *Journal of Geophysical Research: Planets*, 117(E12).

Clemens, J. and Mawer, C. (1992). Granitic magma transport by fracture propagation. *Tectonophysics*, 204(3-4):339–360.

Colon, D. (2018). Understanding the origins of yellowstone hot spot magmas through isotope geochemistry, high-precision geochronology, and magmatic-thermomechanical computer modeling.

Foulger, G. R. and Jurdy, D. M. (2007). *Plates, plumes, and planetary processes*, volume 430. Geological Society of America.

Havlin, C., Parmentier, E., and Hirth, G. (2013). Dike propagation driven by melt accumulation at the lithosphere–asthenosphere boundary. *Earth and Planetary Science Letters*, 376:20–28.

Langmuir, C. H., Klein, E. M., and Plank, T. (1992). Petrological systematics of mid-ocean ridge basalts: Constraints on melt generation beneath ocean ridges. *Mantle flow and melt generation at mid-ocean ridges*, 71:183–280.

Lourenço, D. L., Rozel, A., and Tackley, P. J. (2016). Melting-induced crustal production helps plate tectonics on earth-like planets. *Earth and Planetary Science Letters*, 439:18–28.

Lourenço, D. L., Rozel, A. B., Gerya, T., and Tackley, P. J. (2018). Efficient cooling of rocky planets by intrusive magmatism. *Nature Geoscience*, 11(5):322.

Mahon, K. I., Harrison, T. M., and Drew, D. A. (1988). Ascent of a granitoid diapir in a temperature varying medium. *Journal of Geophysical Research: Solid Earth*, 93(B2):1174–1188.

McKenzie, D., McKenzie, J. M., and Saunders, R. S. (1992). Dike emplacement on venus and on earth. *Journal of Geophysical Research: Planets*, 97(E10):15977–15990.

McLeod, P. and Tait, S. (1999). The growth of dykes from magma chambers. *Journal of volcanology and Geothermal Research*, 92(3-4):231–245.

Mole, D. R., Fiorentini, M. L., Thebaud, N., Cassidy, K. F., McCuaig, T. C., Kirkland, C. L., Romano, S. S., Doublier, M. P., Belousova, E. A., Barnes, S. J., et al. (2014). Archean komatiite volcanism controlled by the evolution of early continents. *Proceedings of the National Academy of Sciences*, 111(28):10083–10088.

Nakagawa, T. and Tackley, P. J. (2012). Influence of magmatism on mantle cooling, surface heat flow and urey ratio. *Earth and Planetary Science Letters*, 329:1–10.

Petford, N., Cruden, A., McCaffrey, K., and Vigneresse, J.-L. (2000). Granite magma formation, transport and emplacement in the earth's crust. *Nature*, 408(6813):669.

Petford, N., Kerr, R. C., and Lister, J. R. (1993). Dike transport of granitoid magmas. *Geology*, 21(9):845–848.

Scott, D. R. and Stevenson, D. J. (1986). Magma ascent by porous flow. *Journal of Geophysical Research: Solid Earth*, 91(B9):9283–9296.

Tackley, P. J. (2008). Modelling compressible mantle convection with large viscosity contrasts in a three-dimensional spherical shell using the yin-yang grid. *Physics of the Earth and Planetary Interiors*, 171(1-4):7–18.

Thybo, H. and Artemieva, I. M. (2013). Moho and magmatic underplating in continental lithosphere. *Tectonophysics*, 609:605–619.

Turcotte, D. and Ahern, J. (1978). A porous flow model for magma migration in the asthenosphere. *Journal of Geophysical Research: Solid Earth*, 83(B2):767–772.

Turcotte, D. L. (1987). Physics of magma segregation processes. In *Magmatic processes: physicochemical principles*, volume 1, pages 69–74. The Geochemical Society, University Park Pennsylvania.

Weinberg, R. F. and Podladchikov, Y. (1994). Diapiric ascent of magmas through power law crust and mantle. *Journal of Geophysical Research: Solid Earth*, 99(B5):9543–9559.